



Uniaxial Compression Study on Mechanical Properties of Artificial Rock Specimens with Cross-Flaws

L. X. Xiong · H. J. Chen · D. X. Geng

Received: 11 November 2019 / Accepted: 25 September 2020 / Published online: 8 October 2020
© Springer Nature Switzerland AG 2020

Abstract Uniaxial compression tests have been performed on artificial rock specimens weakened by feathered with cross-flaws. The effects of the angle α between the primary joint plane and the loading direction, the angle β between the primary joint plane and the secondary joint plane, the length of the primary joint plane, the length of the secondary joint plane, and the number of secondary joint planes on the mechanical behaviors of artificial rock specimens have been studied. Research results show: (1) For artificial rock specimens with two intersecting joint planes of equal length, the uniaxial compressive strength (UCS) is generally higher when the primary and the secondary joint planes are more symmetrically

distributed on both sides of the loading direction. This is mainly due to a shear failure being less likely to occur in this configuration. When the angle β between the primary joint plane and the secondary joint plane remains constant, the UCS of specimens is lowest when the primary joint plane is perpendicular to the loading direction. (2) When the model specimen contains two joint planes and the angle α is the same, the change of the UCS with angle β from 0° to 90° is the same for artificial rock specimens with different lengths of the secondary joint plane. When the angle α and the angle β both remain unchanged, the UCS of the artificial rock specimen decreases with increasing length of the secondary joint plane. (3) When the model specimen contains varied (or equal) lengths of joint planes, the UCS of the specimen decreases with increasing number of secondary joint planes. The UCS does not change substantially when the number of secondary joint planes exceeds 4.

L. X. Xiong (✉)
School of Civil Engineering and Architecture, East China
Jiaotong University, Nanchang 330013, China
e-mail: xionglx1982@126.com

L. X. Xiong
Guangxi Key Laboratory of Disaster Prevention and
Engineering Safety, Guangxi University,
Nanning 530004, China

H. J. Chen
Geotechnical Engineering Department, Nanjing Hydraulic
Research Institute, Nanjing, China
e-mail: hjchen@nhri.cn

D. X. Geng
School of Civil Engineering and Architecture, East China
Jiaotong University, Nanchang 330013, China
e-mail: gengdaxin@ecjtu.jx.cn

Keywords Artificial rock specimen · Cross-flaws · Uniaxial compressive strength (UCS)

1 Introduction

Natural rock fractures and joint planes have a significant influence on the mechanical properties of rock masses. Jointed rocks are commonly observed in construction of various projects, which has been a hot

topic over the last five decades. Therefore, it is of great practical significance to carry out research on the influence of geometrical parameters of joints on the strength and failure modes of jointed rock masses.

Many studies have been reported using compression tests and numerical simulations on rock model specimens containing a single set of parallel joint planes. For example, Manouchehrian and Marji (2012) numerically analyzed the confinement effect on the crack propagation in a pre-cracked rock under compression test. Yang (2011) and Yang et al. (2016, 2018) conducted compression experiments and numerical modeling to evaluate the influence of ligament angle on the strength, deformability, and fracture coalescence behaviors of sandstone specimens containing one single and two joints. Chen et al. (2013) and Cheng et al. (2016) conducted tests and modeled the macro-mechanical behaviors of jointed blocks with high joint density under uniaxial loading, using particle flow code (PFC). Zhang and Wong (2013) studied the cracking processes in rock-like material containing a single flaw and two flaws under uniaxial compression through particle flow modeling. Bahaaddini et al. (2013) numerically investigated the effect of joint geometrical parameters on the mechanical properties of non-persistent jointed rock specimens under uniaxial compression. Li and Wong (2014) numerically studied the coalescence of two pre-existing parallel flaws in rock subjected to uniaxial compression. Huang et al. (2016) investigated the deformation and strength behaviors of sandstone samples with two pre-existing flaws through uniaxial compression tests. Yang et al. (2017) studied the effect of parallel joint interaction on mechanical behavior of jointed rock models under uniaxial compression through laboratory tests and particle flow modeling. Zhao et al. (2016) investigated the cracking and stress–strain behavior of rock-like material containing two flaws under uniaxial compression. Zhou and Bi (2016) conducted 3D numerical study on the growth and coalescence of pre-existing flaws in rock-like materials subjected to uniaxial compression. Cao et al. (2018) also studied the failure patterns of rock-like materials containing multiple joints under compressive-shear test experimentally and numerically.

The above-mentioned tests and numerical results focus only on the mechanical behaviors of rock specimens containing one joint plane or a single set of parallel joint planes. In actual rock engineering,

there may be multiple sets of cross joint planes. Only few scholars have conducted compression tests and numerical simulations of rock specimen containing cross-flaws. Kulatilake et al. (2001) conducted uniaxial compression tests and numerical simulations on rock specimens containing intersecting joint planes. Yin et al. (2016) studied the mechanical behavior, crack initiation stress, cracking modes, and crack coalescence due to uniaxial compressive loading for brittle granite specimens containing two orthogonal fissures. Zhang et al. (2016) carried out uniaxial compression tests on reinforced rock specimens with cross-flaws and with a single flaw. Liu et al. (2018) carried out axial compression tests on rock specimens with different joint geometries (single joint, X-shape cross joint, T-shape cross-joint).

However, the results on the mechanical properties of rock specimens containing cross joint planes are still insufficient to date, and many influence factors still remain unaddressed, such as the angle α between the primary joint plane and the loading direction, the angle β between the primary joint plane and the secondary joint plane, and the influence factors such as the lengths of the primary and secondary joint planes, and the number of secondary joint planes. In this study, we used uniaxial compression tests and numerical simulations to explain the mechanical behaviors of artificial rock specimens with cross joint planes. Then, the effects of the angle α between the primary joint plane and the loading direction, the angle β between the primary joint plane and the secondary joint plane, the length of the primary joint plane, the length of the secondary joint plane, and the number of secondary joint planes on the strength characteristics of artificial rock specimens were studied.

2 Experimental Setup

2.1 Sample Preparation

The samples used in this study have dimensions of 100 mm × 100 mm × 100 mm. Non-persistent joints were modeled by inserting wood planks with thickness of 1 mm into the mold after the model materials. The uniaxial compressive loading diagram of the artificial rock model with cross joints is shown in Fig. 1.

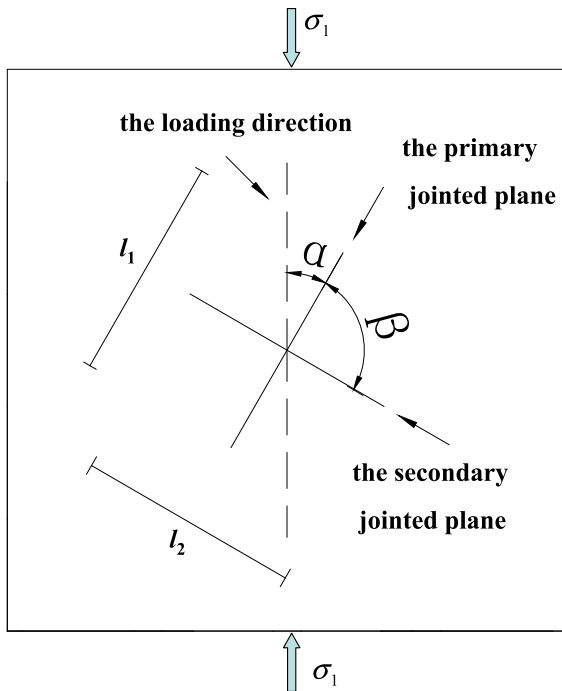


Fig. 1 The uniaxial compressive loading diagram of artificial rock specimen with cross joints

In Fig. 1, the angle α is the angle between the primary joint plane and the loading direction. The angle β is the angle between the primary joint plane and the secondary joint plane. The lengths l_1 and l_2 are respectively the length of the primary joint plane and the length of the secondary joint plane.

Cement mortar was poured into the mold to prepare the specimens for this study. The water/cement ratio is 0.65. Cement No. 425 produced by the China Building Materials Academy was used in this test. Quartz sand was used in the tests. The particle size of sand ranges from 0.5 to 1.0 mm. Wood plank was inserted in the positions of the primary joint plane and the secondary joint plane marked in short-line in Fig. 1 after the initial setting of the cement mortar. The wood planks remain permanently in the specimens. The length of wood planks is 11 mm, this is the same method we used in previous experiments (Xiong et al. 2019a, b).

2.2 Test Procedure

After the test specimens were cured for 28 days and then stored for another 7 days, UCS tests were carried out on these specimens at a displacement loading rate

of 0.6 mm/min. We used WAW-600C universal testing machine to conduct the uniaxial compression tests in this study. A picture and explanation of this machine were presented in Xiong et al. (2019b). The specimens in this study were prepared with the same materials and in the same way as the specimens reported in Xiong et al. (2019b).

According to the angle α , the angle β , the length l_1 and the length l_2 , uniaxial compression test schemes are given in Table 1.

3 Test Results and Analysis

3.1 Variation of Stress–Strain Curves

In this test, the angle α is varied from 0° to 90° . The obtained stress–strain curves for specimens with varying angles β are plotted in Fig. 2.

Figure 2 shows that when α is the same and β increases from 0° to 90° , the stress–strain curves can be divided into four stages, i.e. the compaction stage, linear elastic stage, peak-pre yielding stage and post-peak softening stage. The peak stress at $\beta = 0^\circ$ is higher than that when β is 90° . $\beta = 0^\circ$ indicates the secondary joint coincides with the primary joint.

3.2 Evolution of UCS

When the angle α varies from 0° to 90° , the UCSs of the specimens with various angles β are shown in Fig. 3.

In the range of angle α from 0° to 90° , when the angle α remains unchanged and the value $(\alpha + \beta)$ is less than 90° , the UCS gradually decreases with the increase of angle β . The UCS gradually increases with the increase of angle β when angle α remains unchanged and the value $(\alpha + \beta)$ is greater than 90° , and the UCS is generally higher when the primary and secondary joint planes are more symmetrically distributed on both sides of the loading direction.

This is mainly due to, under uniaxial compression, the shear failure being more likely when $(\alpha + \beta)$ is less than 90° . By contrast, the specimen is not likely susceptible to shear failure when $(\alpha + \beta)$ is greater than 90° .

Xiong et al. (2019b) conducted uniaxial compression tests on six intact specimens without joint planes, and the results showed the value of compressive

Table 1 Uniaxial compression test groups of artificial rock specimens with cross joints

Study	The length l_1 /mm	The length l_2 /mm	The angle $\alpha/^\circ$	The angle $\beta/^\circ$	Number of specimens
1	40	40	0	0, 15, 30, 45, 60, 75 and 90	21
2	40	40	15	0, 15, 30, 45, 60, 75 and 90	21
3	40	40	30	0, 15, 30, 45, 60, 75 and 90	21
4	40	40	45	0, 15, 30, 45, 60, 75 and 90	21
5	40	40	60	0, 15, 30, 45, 60, 75 and 90	21
6	40	40	75	0, 15, 30, 45, 60, 75 and 90	21
7	40	40	90	0, 15, 30, 45, 60, 75 and 90	21

strength are 38.74 MPa, 41.28 MPa, 38.94 MPa, 39.83 MPa, 40.06 MPa and 40.42 MPa, respectively, with the average value of 39.88 MPa. From Fig. 3, the compressive strength of the specimen is significantly reduced when joints are added in the specimen.

When the angle β is the same, the influence of angle α from 0° to 90° on the UCS of specimens is shown in Fig. 4.

The test results show that when the angle β remains constant, the UCS of specimen is lowest when the primary joint plane is perpendicular to the loading direction. Zhang et al. (2012, 2014) found that when the angle β remains constant, the UCS of specimen is lowest when the angle β is 30° to 45° . There is a difference between conclusions in this paper and those obtained by Zhang et al. (2012, 2014), which may be related to the size of the specimen. Zhang et al. (2012, 2014) used rectangular specimens with a size of $70\text{ mm} \times 70\text{ mm} \times 140\text{ mm}$.

3.3 Evolution of Elastic Modulus

When the angle α is the same, the influence of the angle β on the elastic modulus of specimens is shown in Fig. 5.

The test results show that when the angle α is kept constant, there is no regular variation of the elastic modulus with the angle β changing from 0° to 90° .

4 The Comparison between Experimental and Numerical Results

4.1 Numerical Model

The software FLAC^{3D} was used for numerical simulation in this study. The joint plane has no mechanical parameters (Xiong et al. 2019a). The location of the joints is marked as empty in the numerical simulation, and it is filled with wood plank during the laboratory experiment. This is the difference between the numerical simulation and the experiment. The size of the specimen is also $100\text{ mm} \times 100\text{ mm} \times 100\text{ mm}$.

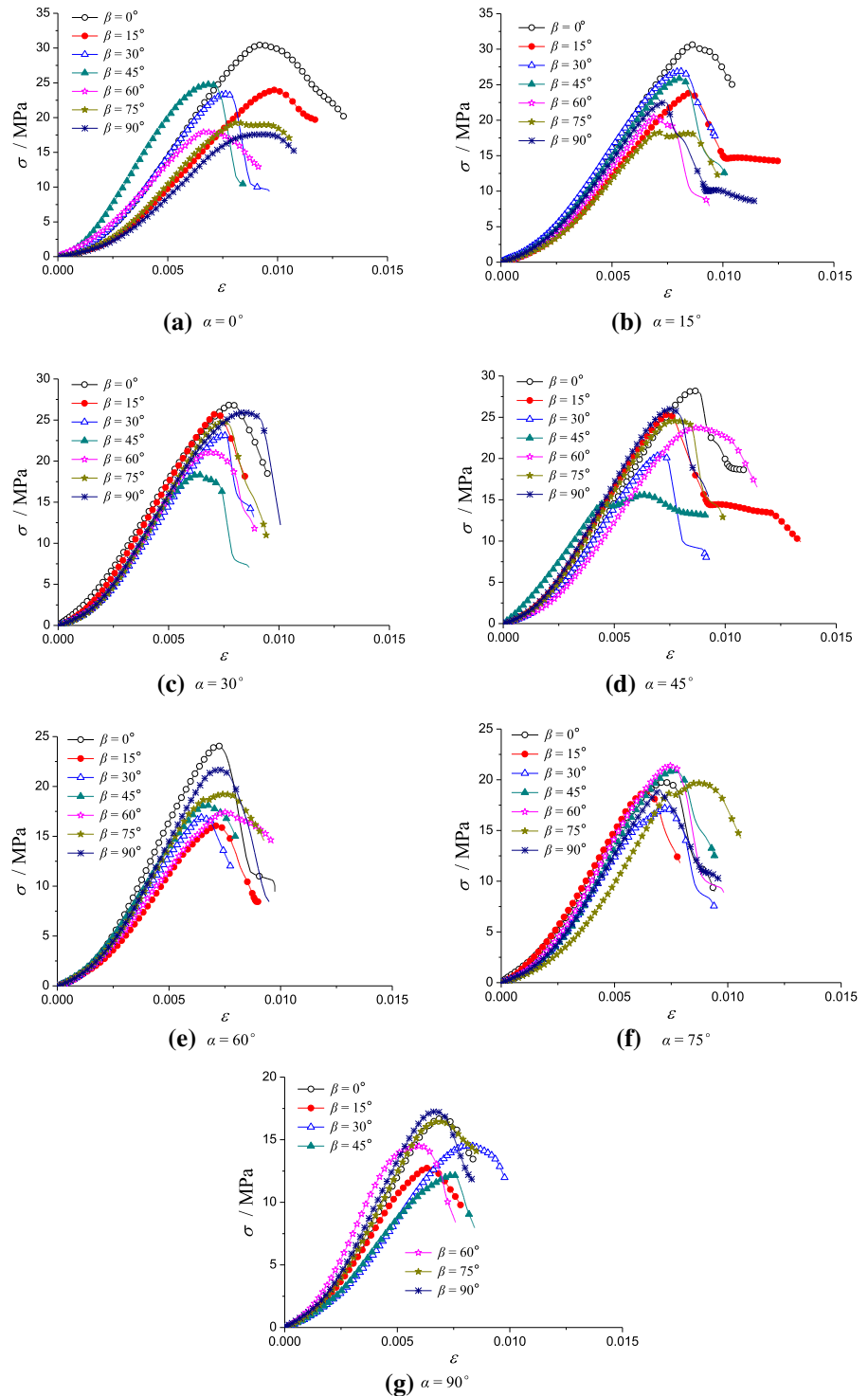
When there are two intersecting joint cracks in the model and the length of joint plane is 40 mm, the model at $\alpha = 45^\circ$ and $\beta = 45^\circ$ is shown in Fig. 6.

4.2 Constitutive Model and Calculation Parameters

Mohr Coulomb model was used in the numerical analysis and calculation parameters for rock-like materials are as follows: bulk modulus K is 8 GPa, the shear modulus G is 4.8 GPa, the cohesion is 5.0 MPa, the internal friction angle is 47° , and the tensile strength is 2.5 MPa.

When we conducted uniaxial compression tests on a small number of specimens, the vertical strain is measured by attached strain gauges to determine the elastic modulus. The preliminary obtained parameters from uniaxial compression tests are used in numerical simulations. If the numerical compression test gives the same result as the experimental test, this parameter was then used in other numerical tests. The calculation

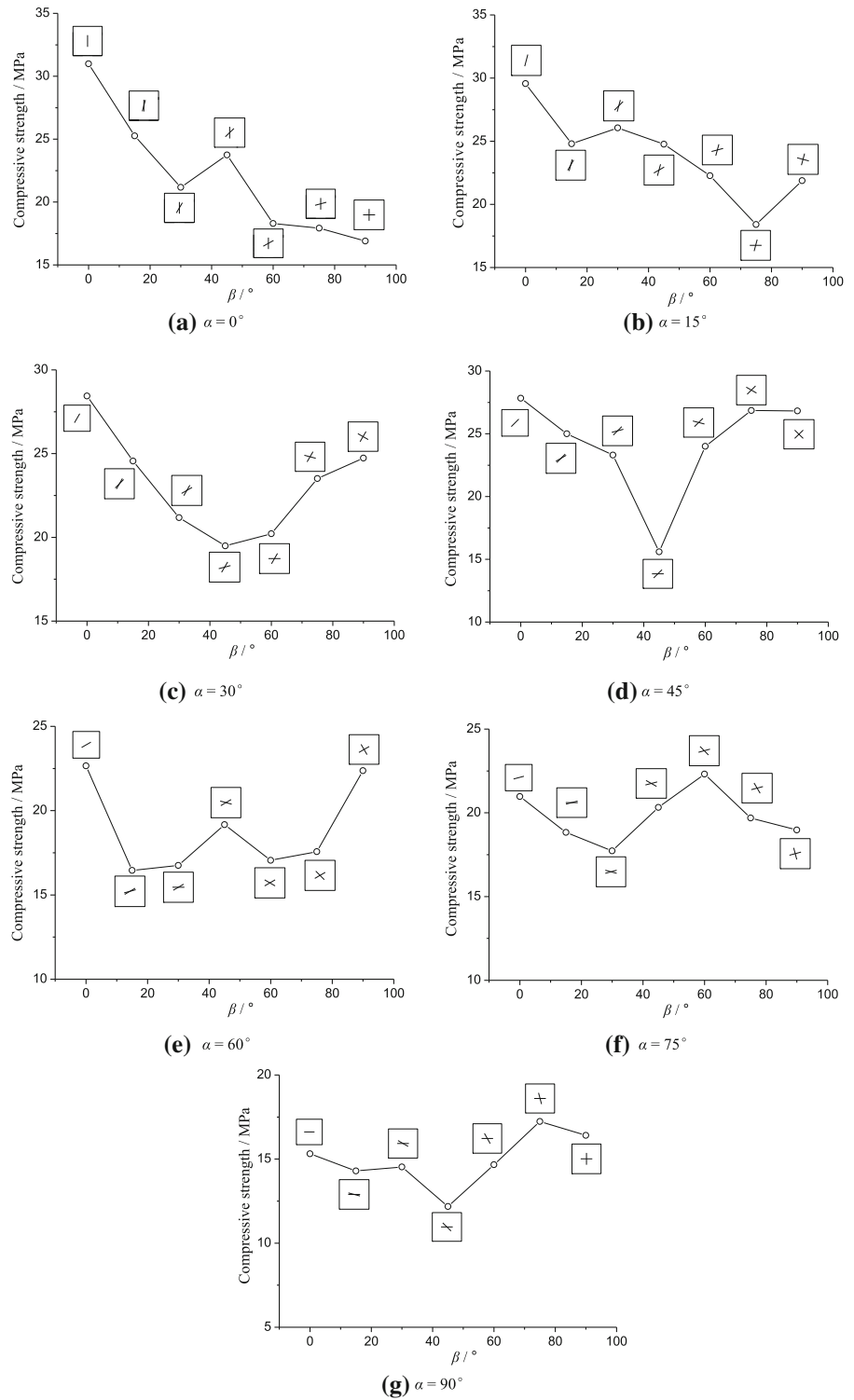
Fig. 2 Influence of angle β on the experimental stress–strain curve of specimen with varied angle α



parameters in this study are consistent with the numerical simulation parameters in our uniaxial

compression tests on artificial rock specimens with two parallel joints (Xiong et al. 2019a).

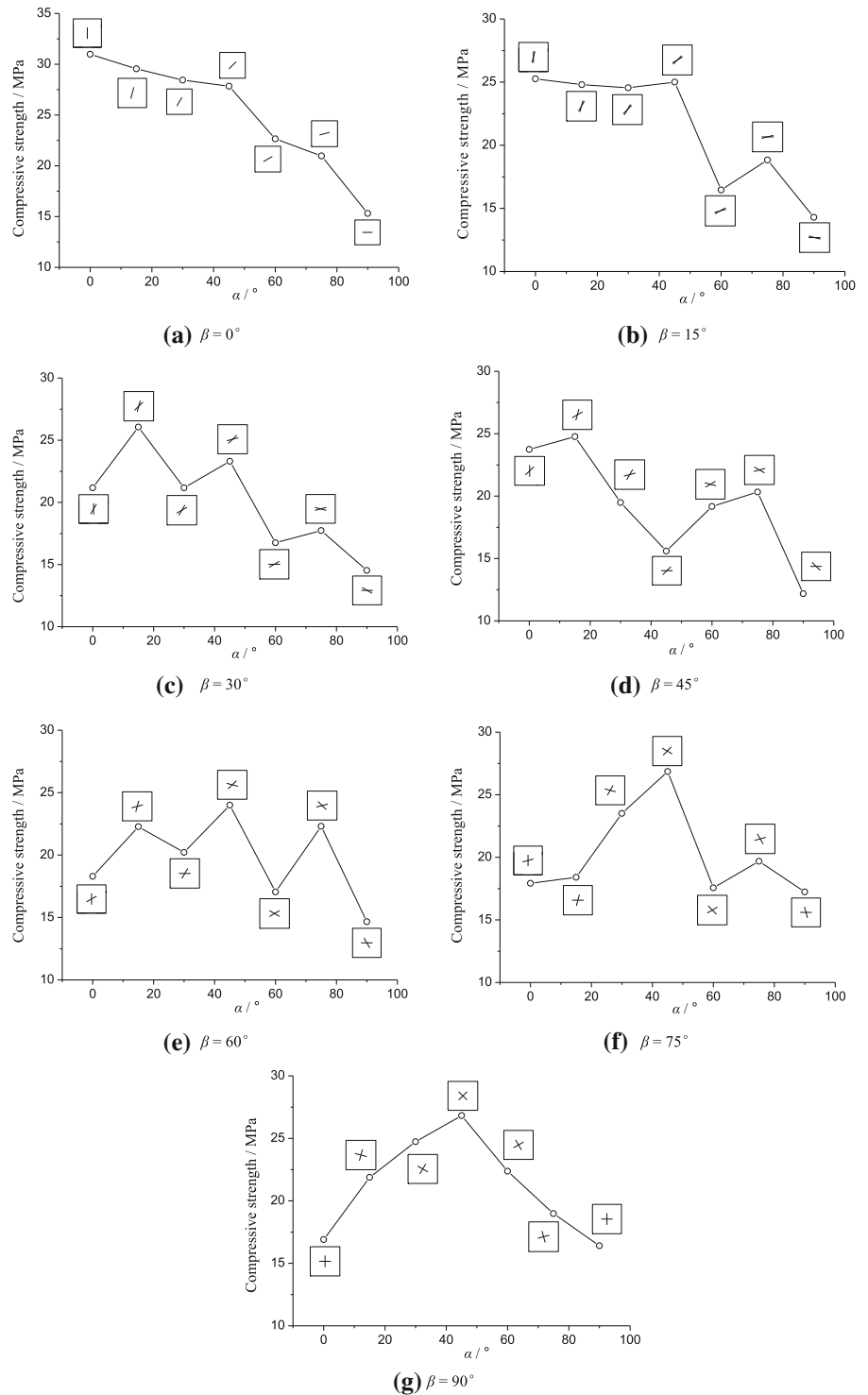
Fig. 3 Influence of angle β on the experimental UCS of specimen when the angle α is the same



In the numerical simulation, vertical constraints were applied on the bottom edge of the model. In this

study, the staged loading method is used regardless of the effect of the loading rate. In the initial loading, the

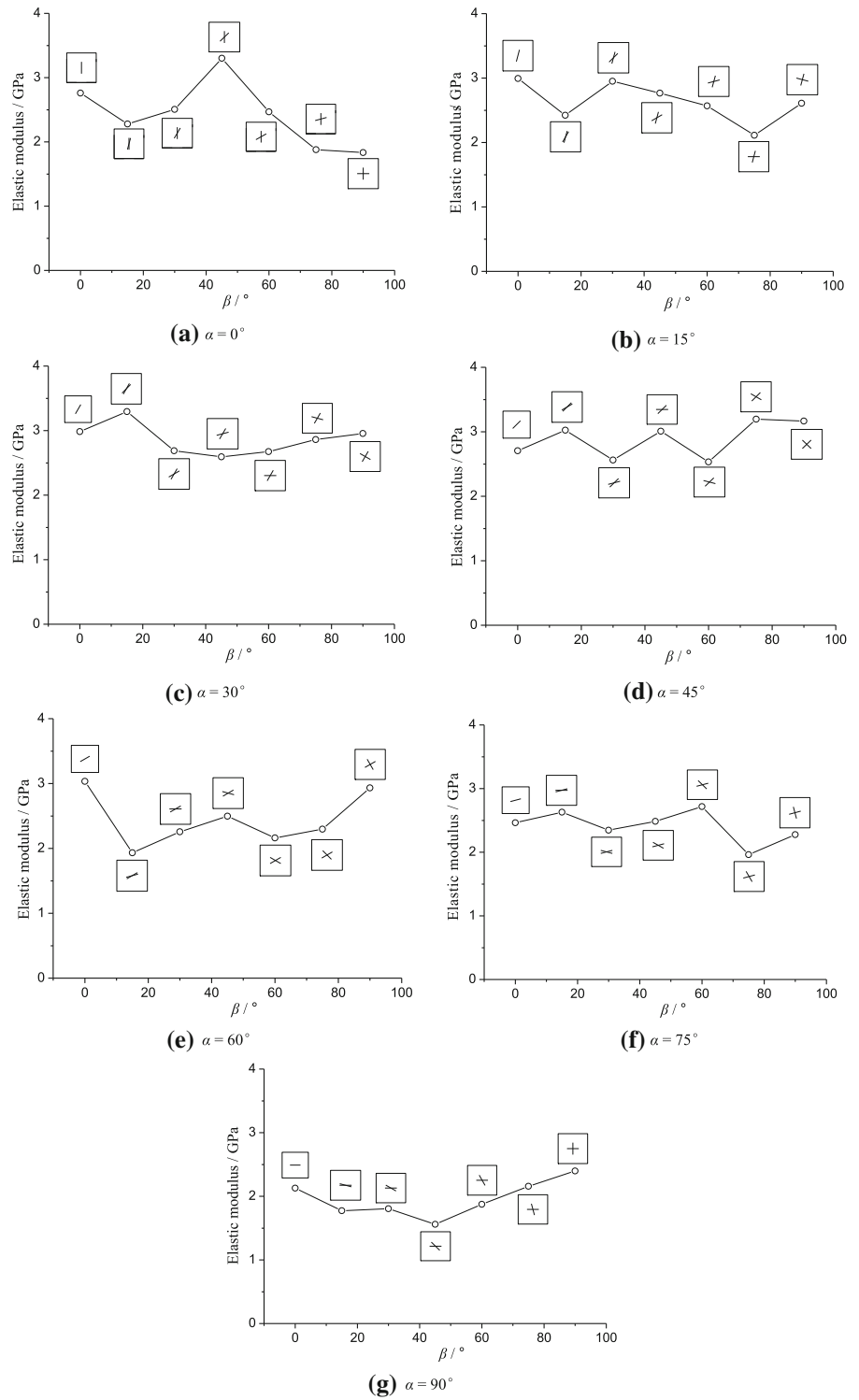
Fig. 4 Influence of angle α on the experimental UCS of specimen when the angle β is the same



stress increment of each stage is 5 MPa. After the strength range was determined, the stress increment was continuously reduced until the calculation cannot

iteratively converge, and this critical stress was set as the compressive strength.

Fig. 5 Influence of angle β on the experimental elastic modulus of specimen when the angle α is the same



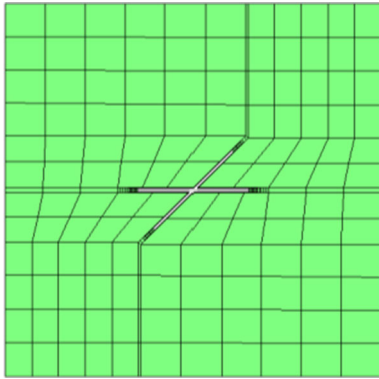


Fig. 6 Numerical models with two joint planes of equal length

Because the Mohr–Coulomb constitutive model was used in this study, only the evolution of the plastic zone is obtained. The evolution of the crack cannot be obtained.

4.3 Comparison of Experimental and Numerical Results

When the angle α is the same, the UCS results, with angle β changing from 0° to 90° , of experimental and numerical results are shown in Fig. 7.

When the angle α is the same, the UCS numerical results are generally lower than experimental results, which is mainly due to the fact that the joint planes were simulated by the empty units in the numerical simulation. Specifically, when the angle α is 45° , 60° , and 75° respectively, the numerical results show little change with the increase of angle β . Despite the differences between the numerical and experimental results with the increase of angle β when α is 90° , the variations of the numerical results, with the increase of angle β , are basically the same as the experimental ones at the angle α of 0° , 30° , 45° , 60° and 75° respectively. Therefore, when α is the same, the change of the numerical simulation results with the increase of β is as a whole the same as that of the experimental results.

5 Numerical Simulation of Jointed Rock Specimens with Two Intersecting Joint Planes

5.1 Numerical Model

In this part, the authors, through numerical simulations, consider the cases when the lengths of the two intersecting joint planes are 20 mm, 40 mm, 60 mm, and 80 mm respectively.

The cases were also considered when the length of the primary joint is kept at 80 mm and the length of the secondary joint is 20 mm, 40 mm, 60 mm, and 80 mm respectively.

5.2 Analysis of Numerical Results

When the angle α is the same and with the increase of the angle β , the UCS evolution of specimens with two joint planes of equal length is shown in Fig. 8.

When α is the same, the UCS of specimens containing different lengths of joint planes is basically the same with the increase of the angle β . When both angle α and angle β are the same, the UCS of specimen decreases with increasing length of joint planes from 20 to 80 mm. This is the same as the numerical simulation conclusion obtained by Ma et al. (2019).

When the angle α is the same and with the increase of the angle β , the UCS of specimens with two unequal length joint planes is shown in Fig. 9.

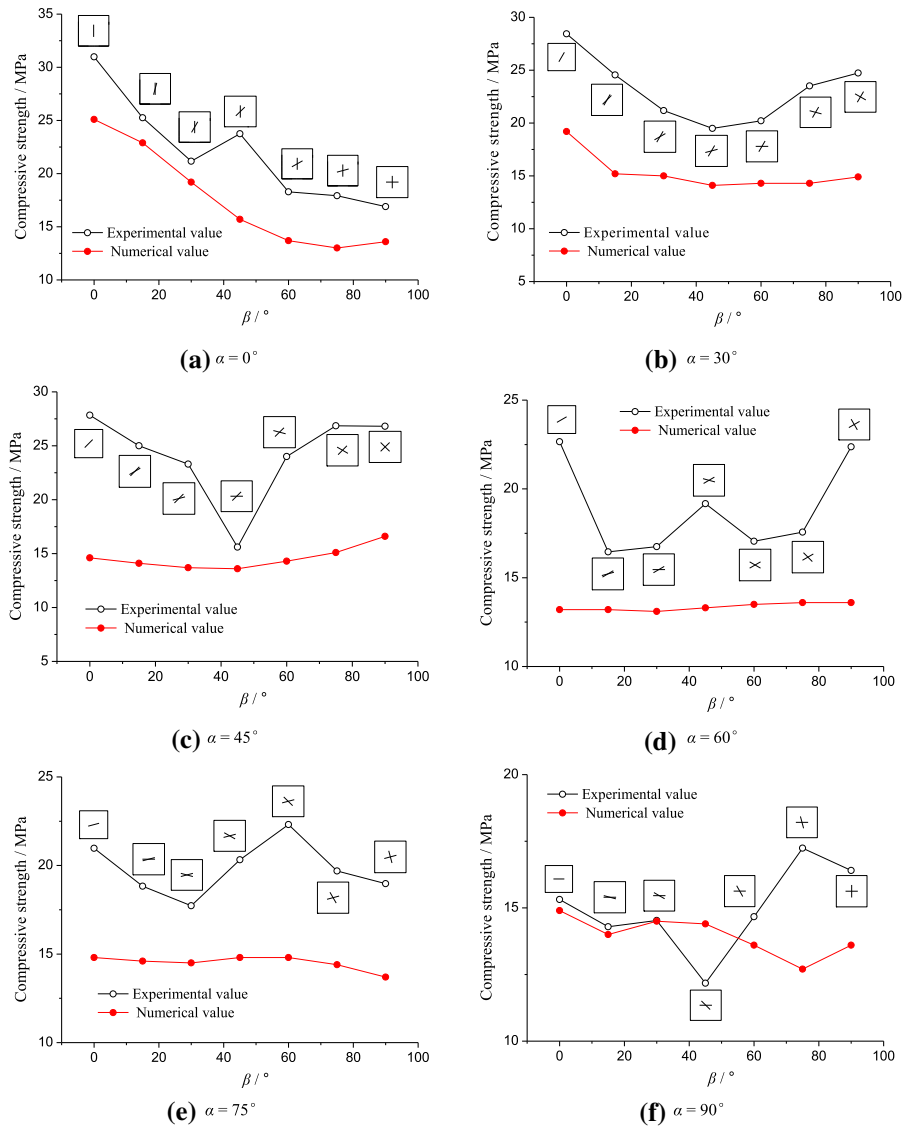
When the angle α is the same with the primary joint plane of unequal length, the UCS of rock specimens containing different lengths of the secondary joint plane is basically the same with the increase of angle β . When the length of the primary joint, the angle α and the angle β are the same, the UCS of the specimen decreases with increasing length of the secondary joint plane from 20 to 80 mm.

6 Numerical Simulation of Jointed Rock Specimens with Multiple Intersecting Joint Planes

6.1 Numerical Model

Numerical simulation of the uniaxial compression test is carried out on a model containing joint planes with equal length. The angles between the two joints in the model are 30° , 45° and 60° . And there are four lengths

Fig. 7 UCS comparison of experimental and numerical results of specimen with two joint planes of equal length



of joint planes, 20 mm, 40 mm, 60 mm, and 80 mm. When the angle between the joint planes is 30° and the length of the joint planes is 40 mm, the numerical calculation model with three joint planes is shown in Fig. 10.

When the numerical simulation of uniaxial compression test is carried out on a model with multiple unequal length joint planes, the angle between the two joint planes in the model is 30°. The length of the primary joint plane in the model is kept at 80 mm, and the lengths of the other secondary joint planes are the same in four groups, namely 20 mm, 40 mm, 60 mm, and 80 mm, respectively.

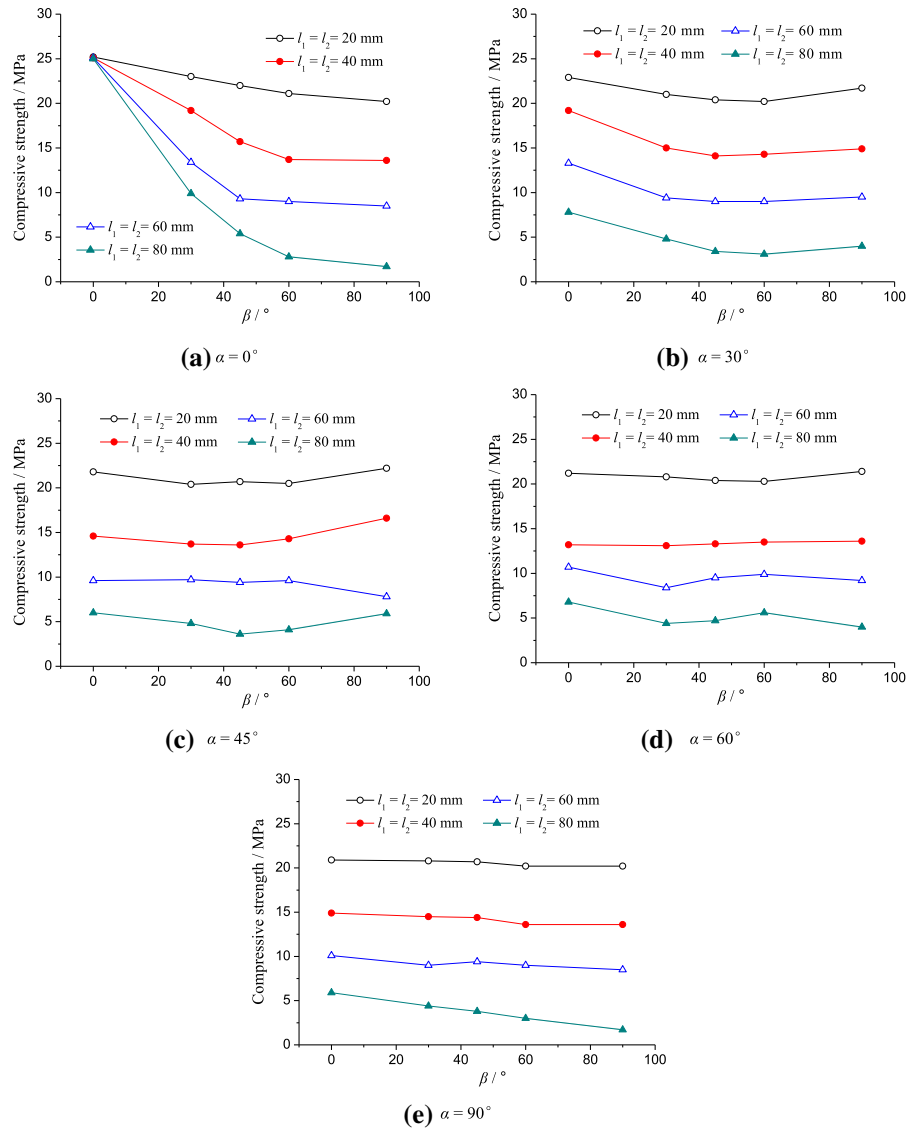
6.2 Analysis of Numerical Results

When the joint planes contained in the model enjoy an equal length, the effect of the number of joint planes on the UCS of specimens is shown in Fig. 11.

The UCS of the model specimens decreases with the increasing number of equal length joint planes. Nevertheless, the UCS does not change substantially when the joint planes outnumber 4.

Based on the same number of joint planes, the UCS of specimen when the angle β_1 is 30° is higher than that when the angle β_1 between the joint planes is 45° and 60°.

Fig. 8 Influence of angle β on the numerical UCS of specimen with two joint planes of equal length when the angle α is the same



When the model contains six unequal length joint planes (the angle between the joint planes is 30°), and the length of the primary joint plane is 80 mm associated with five equal length secondary joint planes, the UCS evolution of the specimen with the increasing number of joint planes is shown in Fig. 12.

In Fig. 12, l_1 is the length of the primary joint plane, and l_2, l_3, l_4, l_5 and l_6 are the lengths of the secondary joint planes.

It can be seen that when the lengths of secondary joint planes in the model are 20 mm, 40 mm, 60 mm, and 80 mm respectively, the UCS of the model specimens decreases with the increasing number of

joint planes. Nevertheless, the UCS does not change substantially when the secondary joint planes out-number 4.

From Figs. 11, 12, when the model contains multiple joint planes with equal or unequal length, the compressive strength of the specimen decreases significantly as the number of joint planes increases from 1 to 3. Zhang et al. (2015) conducted uniaxial compression tests on rock-like material with intersecting multiple flaws, and found that when the length of the secondary joint plane is smaller than the primary joint plane, the number of secondary joint planes has little effect on the compressive strength of the

Fig. 9 Influence of angle β on the numerical UCS of specimen with two unequal length joint planes when the angle α is the same

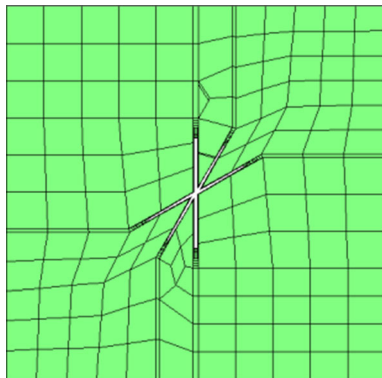
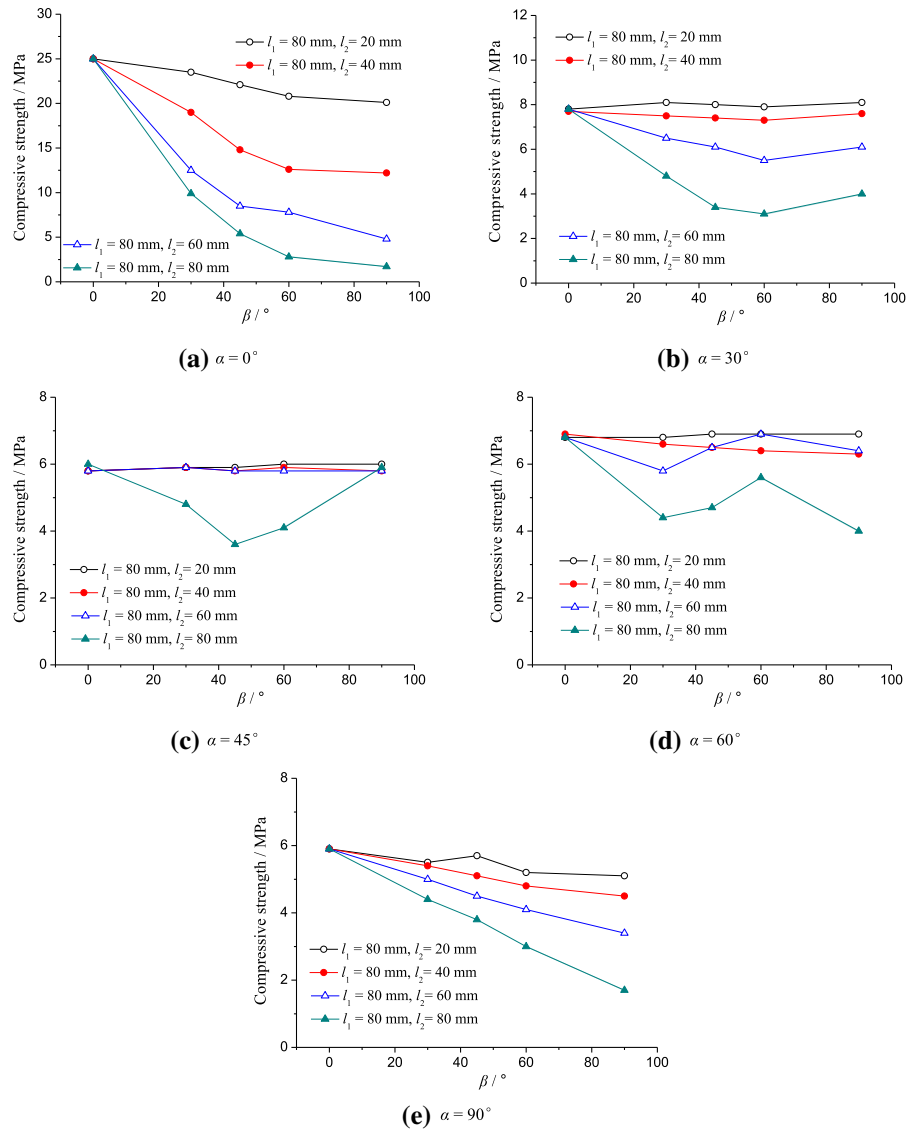


Fig. 10 Numerical models with three equal length joint planes

specimen. When the length of the secondary joint plane was increased to be consistent with the primary joint plane, the increasing number of secondary joint planes has a significant effect on the compressive strength reduction of the specimen. The conclusions obtained through numerical simulation in this study are different from the experimental conclusions of Zhang et al. (2015). We intend to conduct further experimental studies to verify them in the future.

Fig. 11 Effect of the number of joint planes on the numerical UCS of specimen with multiple equal length joint planes

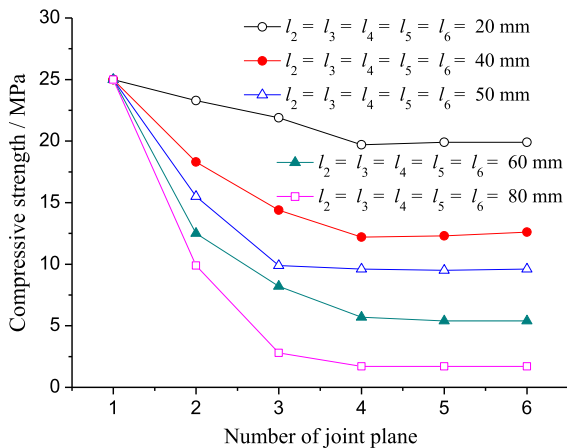
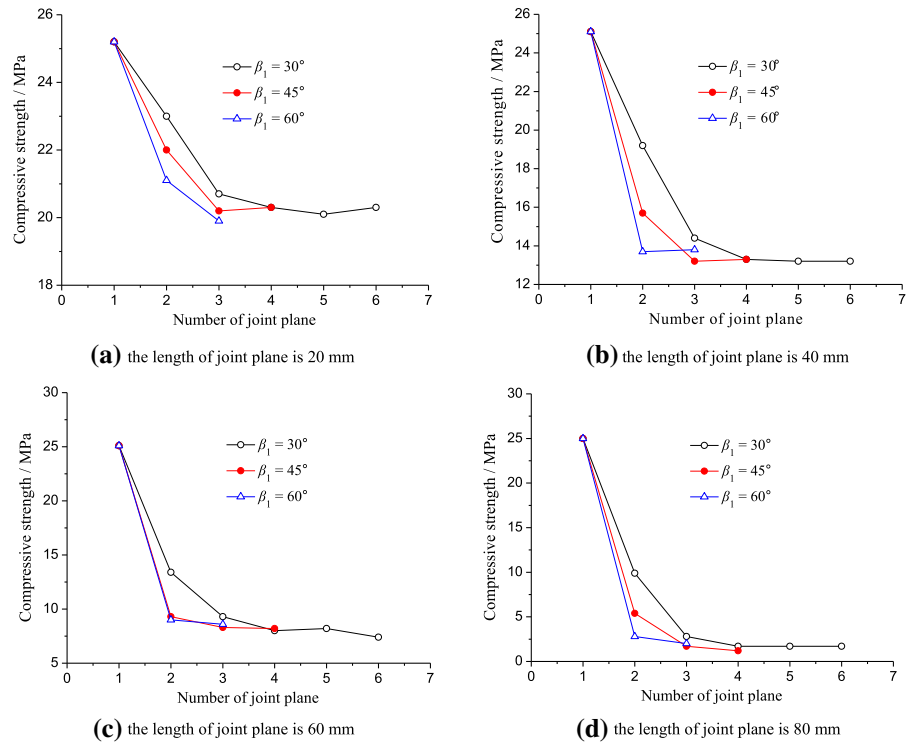


Fig. 12 Effect of the number of joint planes on the numerical UCS of specimen with multiple unequal length joint planes

7 Conclusions

After a series of uniaxial compression tests (UCS) were performed on artificial rock specimens feathered with cross-flaws, the following conclusions are drawn:

(1) For jointed rock specimens with two intersecting joint planes of equal length, the uniaxial

compressive strength (UCS) is generally higher when the primary and the secondary joint planes are more symmetrically distributed on both sides of the loading direction. This is mainly due to the shear failure being less likely to occur in this configuration. When the angle β between the primary joint plane and the secondary joint plane is kept constant and the angle α between the primary joint plane and the loading direction gradually increases, the UCS of specimen is the lowest when the secondary joint plane is parallel to the loading direction with the primary joint plane being perpendicular to the loading direction.

(2) For rock specimens with two intersecting joint planes of equal length, when the angle α between the primary joint plane and the loading direction is kept constant, the elastic modulus of the specimen does not show a regular variation with the angle β between the primary joint plane and the secondary joint plane changing from 0° to 90° .

(3) For rock specimens with two intersecting joint planes of equal length, when the angle α between the primary joint plane and the loading

direction is the same, the UCS evolution of the rock specimens containing joint planes of different lengths with the angle β between the primary joint plane and the secondary joint plane increasing from 0° to 90° is essentially the same. When both the angle α and the angle β are the same, the UCS of the rock specimens decreases with increasing length of joint planes from 20 to 80 mm.

- (4) For rock specimens with two unequal length intersecting joint planes, when both the angle α between the primary joint plane and the loading direction, and the length of the primary joint plane are the same, the UCS evolution of the rock specimens containing secondary joint planes of different lengths with the increase of the angle β between the primary joint plane and the secondary joint plane is the same. When the length of the primary joint plane, the angle α and the angle β are the same, the UCS of the rock specimen decreases with increasing length of the secondary joint planes.
- (5) When the joint planes in the specimen are of equal or unequal length, the UCS of the model specimens decreases with an increasing number of secondary joint planes, however, the UCS does not change substantially when the secondary joint planes outnumber 4.
- (6) When both the number and length of joint planes are the same, the UCS of specimen when the angle between the joint planes is 30° is higher than that when the angle is 45° or 60° .

Due to the low strength of the wood plank, we considered the wood plank as an empty unit in the numerical simulation, also because it is difficult to apply uniaxial compression test on the wood plank to obtain its mechanical parameters. We will furtherly conduct uniaxial and biaxial compression tests on rock-like specimens with cross-cracks, the wood plank will not be left in the specimen in these tests. Furthermore, the PFC program will be used in numerical simulation, the crack evolution law of the rock-like specimens with cross-cracks will be obtained.

Acknowledgements This work was supported by the Systematic Project of Guangxi Key Laboratory of Disaster Prevention and Engineering Safety (Grant No. 2019ZDK051),

and the National Natural Science Foundation of China (Grant No. 41541021).

References

- Bahaaddini M, Sharrock G, Hebblewhite BK (2013) Numerical investigation of the effect of joint geometrical parameters on the mechanical properties of a non-persistent jointed rock mass under uniaxial compression. *Comput Geotech* 49:206–225
- Cao RH, Cao P, Lin H, Ma GW, Zhang CY, Jiang C (2018) Failure characteristics of jointed rock-like material containing multi-joints under a compressive-shear test: experimental and numerical analyses. *Arch Civ Mech Eng* 18:784–798
- Chen X, Liao ZH, Peng X (2013) Cracking process of rock mass models under uniaxial compression. *J Cent South Univ* 20:1661–1678
- Cheng C, Chen X, Zhang SF (2016) Multi-peak deformation behavior of jointed rock mass under uniaxial compression: insight from particle flow modeling. *Eng Geol* 213:25–45
- Huang D, Gu DM, Yang C, Huang RQ, Fu GY (2016) Investigation on mechanical behaviors of sandstone with two preexisting flaws under triaxial compression. *Rock Mech Rock Eng* 49:375–399
- Kulatilake PHSW, Malama B, Wang JL (2001) Physical and particle flow modeling of jointed rock block behavior under uniaxial loading. *Int J Rock Mech Min Sci* 38(5):641–657
- Li HQ, Wong LNY (2014) Numerical study on coalescence of pre-existing flaw pairs in rock-like material. *Rock Mech Rock Eng* 47:2087–2105
- Liu XW, Liu QS, Kang YS, Pan YC (2018) Improved nonlinear strength criterion for jointed rock masses subject to complex stress states. *Int J Geomech* 18(3):04017164(1)–04017164(10)
- Ma P, Xie TC, Liu HY (2019) Numerical analysis of the mechanical behavior of the rock mass with X type cross cracks. *Min Res Dev* 39(2):60–65 (in Chinese)
- Manouchehrian A, Marji MF (2012) Numerical analysis of confinement effect on crack propagation mechanism from a flaw in a pre-cracked rock under compression. *Acta Mech Sin* 28(5):1389–1397
- Xiong LX, Yuan HY, Zhang Y, Zhang KF, Li JB (2019a) Experimental and numerical study of the uniaxial compressive stress–strain relationship of a rock mass with two parallel joints. *Arch Civ Eng* 65(2):67–80
- Xiong LX, Chen HJ, Li TB, Zhang Y (2019b) Uniaxial compressive study on mechanical properties of rock mass considering joint spacing and connectivity rate. *Arab J Geosci* 12:642
- Yang SQ (2011) Crack coalescence behavior of brittle sandstone samples containing two coplanar fissures in the process of deformation failure. *Eng Fract Mech* 78:3059–3081
- Yang SQ, Tian WL, Huang YH, Ranjith PG, Ju Y (2016) An experimental and numerical study on cracking behavior of brittle sandstone containing two non-coplanar fissures

- under uniaxial compression. *Rock Mech Rock Eng* 49:1497–1515
- Yang SQ, Huang YH, Ranjith PG (2018) Failure mechanical and acoustic behavior of brine saturated-sandstone containing two pre-existing flaws under different confining pressures. *Eng Fract Mech* 193:108–121
- Yang XX, Jing HW, Tang CA, Yang SQ (2017) Effect of parallel joint interaction on mechanical behavior of jointed rock mass models. *Int J Rock Mech Min Sci* 92:40–53
- Yin Q, Jing HW, Zhu TT (2016) Mechanical behavior and failure analysis of granite specimens containing two orthogonal fissures under uniaxial compression. *Arab J Geosci* 9:31
- Zhang B, Li SC, Yang XY, Zhang DF, Shao CL, Yang WM (2012) Uniaxial compression tests on mechanical properties of rock mass similar material with cross-cracks. *Rock Soil Mech* 33(12):3674–3679 (in Chinese)
- Zhang B, Li SC, Yang XY, Wang G, Zhang DF, Yang WM, Li JL (2014) Uniaxial compression failure mechanism of jointed rock mass with cross-cracks. *Rock Soil Mech* 35(7):1863–1870 (in Chinese)
- Zhang B, Li SC, Yang XY, Zhang DF, Wang Q, Cai W, Yang CX, Deng ZQ (2015) The uniaxial compression mechanical property of rock-like material with intersecting multi-flaws. *Chin J Rock Mech Eng* 34(09):19–19 (in Chinese)
- Zhang B, Li SC, Xia KW, Yang XY, Zhang DF, Wang SG, Zhu JB (2016) Reinforcement of rock mass with cross-flaws using rock bolt. *Tunn Undergr Space Technol* 51:346–353
- Zhang XP, Wong LNY (2013) Crack initiation, propagation and coalescence in rock-like material containing two flaws: a numerical study based on bonded-particle model approach. *Rock Mech Rock Eng* 46:1001–1021
- Zhao YL, Zhang LY, Wang WJ, Pu CZ, Wan W, Tang JZ (2016) Cracking and stress–strain behavior of rock-like material containing two flaws under uniaxial compression. *Rock Mech Rock Eng* 49:2665–2687
- Zhou XP, Bi J (2016) 3D Numerical study on the growth and coalescence of pre-existing flaws in rocklike materials subjected to uniaxial compression. *Int J Geomech* 16(4):04015096(1)–04015096(20)

Publisher's Note Springer Nature remains neutral with regard to jurisdictional claims in published maps and institutional affiliations.